



Effect of selenium incorporation on the structure and in vitro bioactivity of 45S5 bioglass

Burcu Karakuzu-İkizler¹ · Pınar Terzioğlu² · Bilge Sema Oduncu-Tekerek³ · Sevil Yücel¹

Received: 3 December 2018 / Revised: 30 May 2019 / Accepted: 21 June 2019 / Published online: 2 July 2019
© Australian Ceramic Society 2019

Abstract

In vitro bioactivity, biodegradation, and biocompatibility behavior of a new bioactive glass systems were investigated with the incorporation of selenium oxide, for the replacement of sodium oxide in the traditional 45S5 bioglass composition. The apatite-forming ability of melt-derived bioactive glasses was evaluated by immersion studies in simulated body fluid while monitoring the concentration of silicon, calcium, phosphorus, sodium, and selenium in the medium. The weight loss of bioactive glasses and pH change in the tris-(hydroxymethyl)-amino methane buffer solution was determined to observe the biodegradation behavior of glass samples. The glasses were characterized by a Fourier transform infrared spectroscopy, scanning electron microscopy, inductively coupled plasma, and Vickers hardness measurements. The biocompatibility evaluation of the glasses was determined through in vitro osteogenesis assays by cell viability, alkaline phosphatase activity, and mineralized matrix formation. The incorporation of selenium enhanced the hydroxyapatite formation on the bioactive glass surface and microhardness of glasses. The hardness of glasses was found to decrease with immersion duration. The results indicate that selenium incorporated bioactive glasses can be used as bioactive material in bone tissue engineering applications.

Keywords Alkaline phosphatase · Biodegradation · Hydroxyapatite · Melt-derived bioactive ceramic · Selenium

Introduction

Various kinds of biomaterials have been developed for bone tissue replacement. They need to be stable for long period of time and firmly fixed to the bone [1, 2]. Most biomaterials indicate inert response when implanted in the body; however, bioactive glasses give positive responses by converting to hydroxyapatite which is natural bone substance. Thanks to that, bioactive glasses have been used by the superiority of their capability to bond with

tissues and to support bone formation [3]. Hench et al. proved that bioactive glass (45% SiO₂, 24.5% CaO, 24.5% Na₂O, and 6% P₂O₅) was able to bond to living bone due to the formation of a hydroxyapatite layer on its surface [4]. This layer assists the adhesion of tissues and allows an intimate bonding between bone and implants [5].

The successful interaction of bioactive glass with living tissues is the main goal of biomaterial developments [Hench 2010]. The chemical composition of bioactive glass has a significant effect on binding and the ability of bone-cell proliferation. In general, conventional bioactive glass is composed of silica, calcium, phosphate, and sodium [6, 7]. In the last few years, there has been an increasing interest in the incorporation of various elements as aluminum [8], boron [9], copper [10], magnesium [11], and strontium [12] in the glass network for the synthesis of bioactive glasses with enhanced properties. In this way, bioactive glasses with multifunctional features can be obtained for bone tissue regeneration practices [13]. Among these elements, selenium (Se) is a trace element which naturally found in animal and human tissues. Selenium has been reported to exhibit beneficial biological effects

✉ Pınar Terzioğlu
pinar.terzioglu@btu.edu.tr

✉ Sevil Yücel
yuce.sevil@gmail.com

¹ Bioengineering Department, Faculty of Chemistry and Metallurgy, Yıldız Technical University, Istanbul, Turkey

² Department of Fiber and Polymer Engineering, Faculty of Engineering and Natural Sciences, Bursa Technical University, Bursa, Turkey

³ Genetics and Bioengineering Department, Faculty of Engineering and Architecture, Nişantaşı University, Istanbul, Turkey

as antibacterial [14], antiapoptotic [15], anticancer [16], as well as antioxidant [17] activities. Moreover, studies have shown that selenium-incorporated hydroxyapatite [14, 18], nano-selenium-coated titanium [16], and nanostructured selenium compacts [19] can be used as potential biomaterials for bone repair applications.

Despite the studies, there is a lack of information available in the world literature on the production of selenium incorporated melt-derived bioactive glass. Therefore, the aim of the present study is the preparation and characterization of selenium-incorporated bioactive glasses. Various bioglasses were prepared by replacing selenium (0.75, 1.5, 3, 6 wt.%) with sodium in the 45S5 bioglass system. The hardness and morphology of bioactive glasses were characterized using Vickers hardness measurements and SEM analysis, respectively. In addition, *in vitro* assays were performed to examine biological activities in simulated body fluid (SBF) at different durations (7–28 days), biodegradation behavior in the TRIS solution, and also cell viability, alkaline phosphatase (ALP) activity, and mineralized matrix formation.

Materials and methods

Materials

SiO₂ (Riedel-de Haen), CaCO₃, Na₂HPO₄·2H₂O, NaHCO₃ (Merck), and SeO₂ (Sigma Aldrich) as starting materials for preparation of bioactive glass and reagent-grade chemicals NaCl, NaHCO₃, KCl, Na₂HPO₄·2H₂O, MgCl₂·6H₂O, CaCl₂·2H₂O, Na₂SO₄ trishydroxymethyl aminomethane [Tris-buffer, (CH₂OH)₃CNH₂], and HCl as required materials for preparation of SBF, were purchased from Merck.

Preparation of glasses

The bioactive glasses with the compositions that are given in Table 1 were synthesized through melting process [20, 21]. The CaCO₃, Na₂HPO₄·2H₂O, NaHCO₃, SeO₂, and SiO₂ were

grinded twice in a mortar to provide homogeneity. For each type of bioactive glass batch, the mixture was put into a platinum pot and heated at 1400 °C for an hour. After an hour, the solution was rapidly poured into distilled water to prevent crystallization and filtrated. The bioactive glasses were dried in the oven at 150 °C. The grinding step was repeated to provide homogeneity. The grinded bioactive glass was put into the platinum pot and was heated at 1450 °C for 2 h. The solution was poured into a metal vessel and annealed at 550 °C. After 2 h, the furnace was turned off and has been waited until the bioactive glasses cooled down.

The hydroxyl carbonate apatite (HCA) formation on the bioactive glass surfaces was investigated after immersion in SBF (pH = 7.4, 37 °C) for 7, 14, 21, and 28 days. The SBF was prepared with an ion concentration of Na⁺ 142.0, K⁺ 5.0, Ca²⁺ 2.5, Mg²⁺ 1.5, Cl⁻ 125.0, HPO₄²⁻ 1.0, HCO₃⁻ 27.0, SO₄²⁻ 0.5 mmol/L in the distilled water [11, 21]. The SBF was refreshed for every week during the experimental study.

Characterization of bioactive glasses

The morphology of the bioactive glass samples was assessed using a SEM instrument (JEOL JSM 5410 LV, Japan). The micrographs were obtained using the parameters as EHT = 1.00 kV, WD = 10.0–15.0 mm, and Signal A = SE1.

The concentration changes of silicon, calcium, phosphorus, sodium, and selenium ions in SBF were analyzed using an ICP system (Perkin Elmer Optical Emission Spectrometer Optima 2100 DV, USA).

The functional groups of samples before and after exposure to the SBF were determined by using a Fourier transform infrared spectrometer (Perkin Elmer Spectrum One), in the range of 650–4000 cm⁻¹.

The hardness of the bioactive glass samples were achieved by use of Vickers hardness equipment (Microbul-1000D). The indentations were made within 10 s from the loading 500 gf. The measurements were carried out in triplicate and the results were given as mean ± standard deviation.

In vitro degradation studies

The *in vitro* biodegradation of the bioactive glass samples was assessed by their dissolution behavior in tris-(hydroxymethyl)-aminomethane buffer solution at 37 °C during a week for each day. The tris-(hydroxymethyl)-aminomethane was mixed with distilled water, and the pH of the solution was adjusted to eight with 1 M HCl solution to prepare TRIS buffer solution. TRIS buffer does not contain free ions, thereby provides an environment for maximum dissolution of the bioactive glass. The measurements of pH variations of the buffer solution and weight changes of the samples were executed.

Table 1 Chemical compositions of selenium incorporated melt-derived bioactive glasses

Notations	Chemical Composition of Components (wt.%)				
	SiO ₂	Na ₂ O	CaO	P ₂ O ₅	SeO ₂
B0	45	24.5	24.5	6	–
B1	45	23.75	24.5	6	0.75
B2	45	23	24.5	6	1.5
B3	45	21.5	24.5	6	3
B4	45	18.5	24.5	6	6

In vitro cell studies and alkaline phosphatase activity

Preparation of bioactive glass conditioned medium

Bioglass conditioned medium was prepared as previously described [22]. Briefly, the powdered bioglass (0.1 g) was incubated in 5 mL of serum-free Dulbecco's Modified Eagle Medium/Nutrient Mixture F-12 (DMEM-F12) at 37 °C for 24 h to obtain a bioactive glass conditioned medium with a concentration of 20 mg/mL (powder/DMEM-F12). At the end of 24 h, the mixture was centrifuged. The supernatant was collected, and filtered through a 0.20- μ m filter (Sartorius, UK). The elemental concentration of ions of final solutions was analyzed using the ICP-OES.

Cell culture

Prior to experiments, the SAOS-2 osteoblast-like cells were cultured in DMEM-F12 with 10% fetal bovine serum (FBS) at 37 °C and 5% CO₂. Subsequent media exchanges were made every 2 days.

Cell viability and cytotoxicity studies

Cell viability was measured calorimetrically by the MTT assay in accordance with the manufacturer's protocol (Sigma USA). Cells were placed onto 96-well plates at the density of 10³ cells/well and incubated for 24 h. At the end of incubation, bioactive glasses were added at different concentrations. MTT solution (5 mg/mL, 20 μ L) was added to each well after 24 h and 7 days. DMSO (100 μ L) was added after additional incubation for 4 h. The absorbance values were measured using a microplate reader (Biotek synergy, USA) at 495 nm.

Osteoblast differentiation and mineralization assays

SAOS-2 cells were cultured in osteo-inductive conditioned medium for 7 and 14 days to examine osteoblast differentiation and mineralization assays. Osteoblast differentiation and mineralization were induced by the osteo-inductive conditioned medium. The medium was composed of 10% FBS DMEM containing 50 μ g/mL L-ascorbic acid and 10 mM β -glycerophosphate. Cells treated with 10% FBS DMEM normal medium served as control groups.

Alkaline phosphatase activity assays

The substrate, p-nitrophenyl phosphate, was used to determine alkaline phosphatase (ALP) activity. The 6-well plates were seeded with a suspension containing 2×10^5 SAOS-2 cells/well and allowed at each designated time (7–21 days). The obtained cells were sonicated for 10 min for complete lysis of cells. After centrifugation for 10 min, the supernatants were

collected to be used as samples for the ALP activity assay. The protein concentrations were determined using the bicinchoninic protein assay reagent. The relative activity of the sample is reported as the ratio of activity and the corresponding protein concentration (U/mg).

Matrix mineralization assay

Arsenoz-III staining was used to determine calcified nodule formation. The mineralization assay was performed as previously described [22]. The optical densities monitored by following absorption at 600 nm. The protein from Pierce, Rockford, IL, bicinchoninic acid which was used for the colorimetric detection of the cuprous cation was used to evaluate the total protein content. The calcium content of the cell layer has been normalized to protein content. Additionally, cell cultures were stained with Alizarin red to determine the formation of calcium crystals in the mineralization analysis. The cells were monitored using inverted microscopy (Olympus CKX41).

Results and discussion

Scanning electron microscopy analysis

According to Kokubo et al. [23], it is feasible to investigate the possible precipitation of hydroxyapatite on the surface of a biomaterial by immersion in SBF to estimate its in vivo biological activity. Therefore, the selenium-doped bioglasses were immersed in SBF as preliminary screening of bioactivity.

Micrographs of all bioactive glass samples before and after immersion in SBF solution up to 28 days were investigated to determine the microstructural evaluation of samples. Figure 1 shows the micrographs of bioactive glass samples. The surfaces of bioactive glass samples were smooth and glassy before immersion in SBF solution (figure not given). According to the SEM micrographs, after immersion in SBF, an alteration in surface morphology was observed when compared with the initial surface of the bioglasses. After 7 days, the surfaces of all the bioactive glass samples were covered by apatitic crystals (Fig. 1). The circular hydroxyapatite structure formation was more in the surface cover of B2 and B3 samples as against surfaces of other bioactive glass samples. The morphology with circular particles indicates the presence of characteristic apatite crystals [24–26]. In general, precipitation of apatitic crystals initiates with the generation of sole granules and then dense layer forms on the surface of bioglass by the progressive grow of granules [27]. After 28 days, the surface covering layer of B0, B3, and B4 samples was fractured showing the formation of an amorphous calcium phosphate layer [28]. Gu et al. also observed the same phenomenon and explained that diffusion and reaction between the SBF and the glass surface

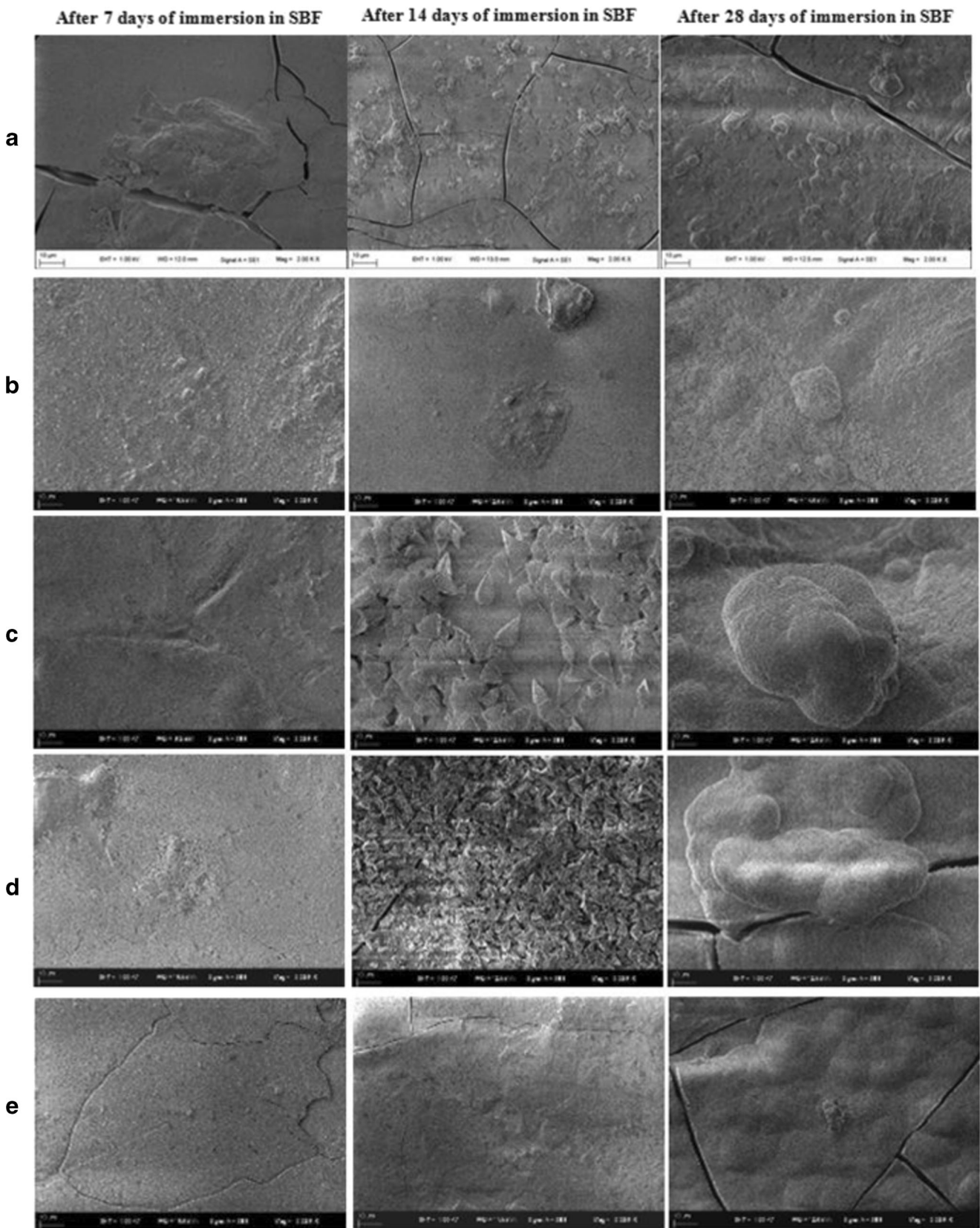


Fig. 1 SEM micrographs of selenium-incorporated glass samples after immersion in SBF up to 28 days **a** B0, **b** B1, **c** B2, **d** B3, **e** B4 ($\times 2000$)

resulted in crack formation [29]. Therewithal, the formation of cracks which is also the evidence of biodegradation can be explained by the rapid release of ions from bioglass after immersion in SBF solution. The formation of HCA layer increased steadily with the increment in immersion time from 7 to 28 days. These features demonstrated that the selenium-incorporated bioglass samples (B1–B4) had the potential of bone-like apatite layer formation on their surfaces promoting the ability of bone bonding with living tissues.

ICP analysis

Since 1987, simulated body fluid has been used to determine the in vitro bioactivity of biomaterials [30, 31]. In this study,

the bioactivities of glasses were also evaluated in SBF and compared with the control sample. Figure 2a–e represents the change of ion concentrations (Si^{4+} , Ca^{2+} , Na^+ , P^{5+} , and Se^{4+}) between glasses and SBF as a function of immersion time. The change of ion concentrations revealed that all of the bioglasses were bioactive.

The decrease of Ca^{2+} concentration in SBF supported the calcium phosphate layer formation which was explained by Yan et al. [32]. The calcium ion concentration is checked by the release of Ca^{2+} from the bioactive glass and the hydroxycarbonate apatite (HCA) or phosphate formation. P^{5+} together with Ca^{2+} involves in the structure of calcium phosphate which results in the formation of hydroxycarbonate apatite. The HCA layer occurs after the calcium phosphate

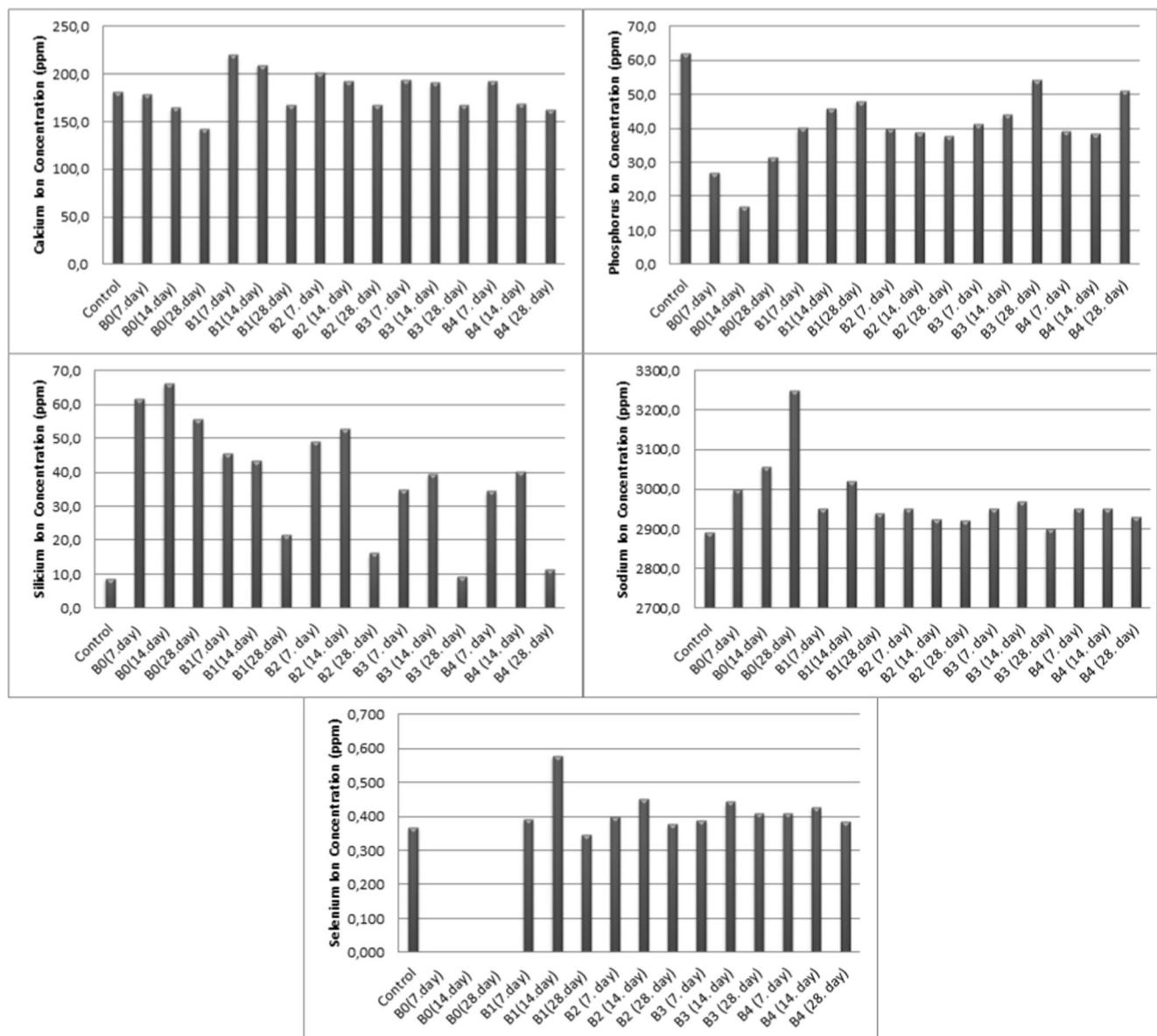


Fig. 2 The change of ion concentrations between glasses and SBF at 7–28 days, **a** Ca ion changes, **b** P ion changes, **c** Si ion changes, **d** Na ion changes, **e** Se ion changes

layer formation on bioactive glass surface due to the adsorption of increased Ca^{2+} and PO_4^{3-} ions in SBF solution.

The Ca^{2+} ion release from all bioglass samples progressively decreased week by week. Combined with the decrease of the P^{5+} concentration in SBF, it was indicating the formation of calcium phosphate layer. It should be noted that the decrease of phosphate ions in SBF was highest at 14th day for B0 when it was highest at 7th day for B1 and B3 samples. However, the P^{5+} concentration in SBF increased for all samples except B2 at 28th day. The decrease of phosphate ions in SBF was continuous for B2 sample. As a result, it can be suggested that besides the selenium-incorporated samples, the 1.5 wt.% selenium incorporation (B2 sample) enhanced the HCA formation and thus bioactivity of bioactive glass. The final Ca^{2+} and P^{5+} concentration in SBF was higher for B1–B4 samples when compared to B0 sample. This was the evidence that the HCA layer formation of selenium incorporated samples (B1–B4) was continued over 28 days and it means those glasses need more time to fully cover with HCA layer by multiple times compared to B0 sample.

Analysis of silicon ion concentration clearly showed that Si^{4+} ion concentration in all of the SBFs increased every after immersion period. The Si^{4+} ion concentration in SBF at 14th day was higher than the other times for most of the glasses (B0, B2–B4). In addition, the Si^{4+} ion release decreased with an increase in the ratio of selenium addition and time. The reduction of Si^{4+} ion release during time might be due to the deceleration of dissolution process through the precipitation of the phosphates or silicates [24]. The Si^{4+} release was higher for B1 sample than B2–B4 samples.

Se^{2-} ion release of all samples was very similar. Only the concentrations of Se^{2-} ions in B1 immersed SBF sample were a little higher (~ 0.1 ppm) than the others after 14 days.

Sodium ion release is also an indicator of glass dissolution. It can be seen that there was sodium ion release from all of the bioactive glasses. However, it was less for selenium-incorporated bioactive glasses (B1–B4) than B0 sample. These results are in a harmony with weight loss analysis in SBF (Fig. 4). It can be seen that weight loss of B0 sample was higher than B1–B4 samples. It can be concluded from ion release analysis that selenium addition to the glass network slightly decreased the dissolution behavior of glass.

FT-IR analysis

FT-IR analysis was used to monitor the changes of specific chemical groups in the bioactive glass samples before and after immersion in SBF solution. The FT-IR spectrums of bioactive glass sample are shown in Fig. 3. In Fig. 3, the peak at 779 cm^{-1} was due to the Si–O–Si stretching vibrations. The peak observed at 1022 cm^{-1} was a phosphate group (PO_4^{3-}) (Fig. 3a). The peaks at 1650 cm^{-1} and $3000\text{--}3700\text{ cm}^{-1}$ were

related to the H–OH bending vibrations of the water molecules [33].

In Fig. 3b, the bands between 950 and 1050 cm^{-1} were due to the P–O bending vibrations in hydroxyapatite crystalline lattice. The absorption bands at 1411 cm^{-1} and 1458 cm^{-1} were assigned to carbonate group (CO_3^{2-}) that were evidence of HCA layer formation on the surface of samples [34]. The peaks at 1640 cm^{-1} and between 3000 and 3600 cm^{-1} were related to the H–OH bending vibrations of the water molecules.

The peak intensity changes occurred with development of HCA layer which lead to the weakening of the peak attributed to Si–O–Si vibration of bioglass [35]. The peak intensity changes of B2 sample were clearly more than the other samples. Herewith, the FT-IR results indicated that the B2 sample had the highest bioactivity which was also supported by ICP and Vickers hardness analyzes results.

Weight variation of the bioactive glasses

The variation of weight is related to the formation of HCA layer on bioactive glass (weight gain) and dissolution of the glass (weight loss) [36]. Therefore, the amount of HCA layer formation could be predicted by comparing the difference of weight loss after immersion in SBF and TRIS solution. Figure 4 presents the weight loss (%) of the glasses after immersion in SBF and TRIS solution. The dissolution behaviors of glasses were differed related to the solution type. The dissolutions of selenium-incorporated samples (B1–B4) in SBF were a little less than the selenium-free sample (B0). However, according to immersion in TRIS solution results (Fig. 4), the weight change of B2 sample was clearly greatest and followed by B1 sample which showed the higher ion release from these samples. The selenium incorporation increased the weight loss till 3 wt.% Se addition. The dissolution behavior of B4 (6 wt.%) sample was very similar to the B0 sample.

pH variation of the Tris solution

The pH variation of TRIS solution also gives information about the bioactivity behavior of bioglass. Figure 5 presents the pH variation of TRIS solution after immersion of the bioglass samples against time. As previously shown in the literature, the pH of TRIS solution increased by immersion of bioglasses related to the release of ions from glass surface [36, 37]. The released Ca^{2+} and Na^+ ions from the bioglasses replaced with H^+ and H_3O^+ ions from the medium [38]. Additionally, pH increases because of high alkalinity of Na^+ ion [39]. As pronounced, the higher increment of pH pointed out higher reactivity of bioglass [36].

Obviously, with the increase of immersion time, the pH of TRIS solution increased. As can be seen from Fig. 5, the ion

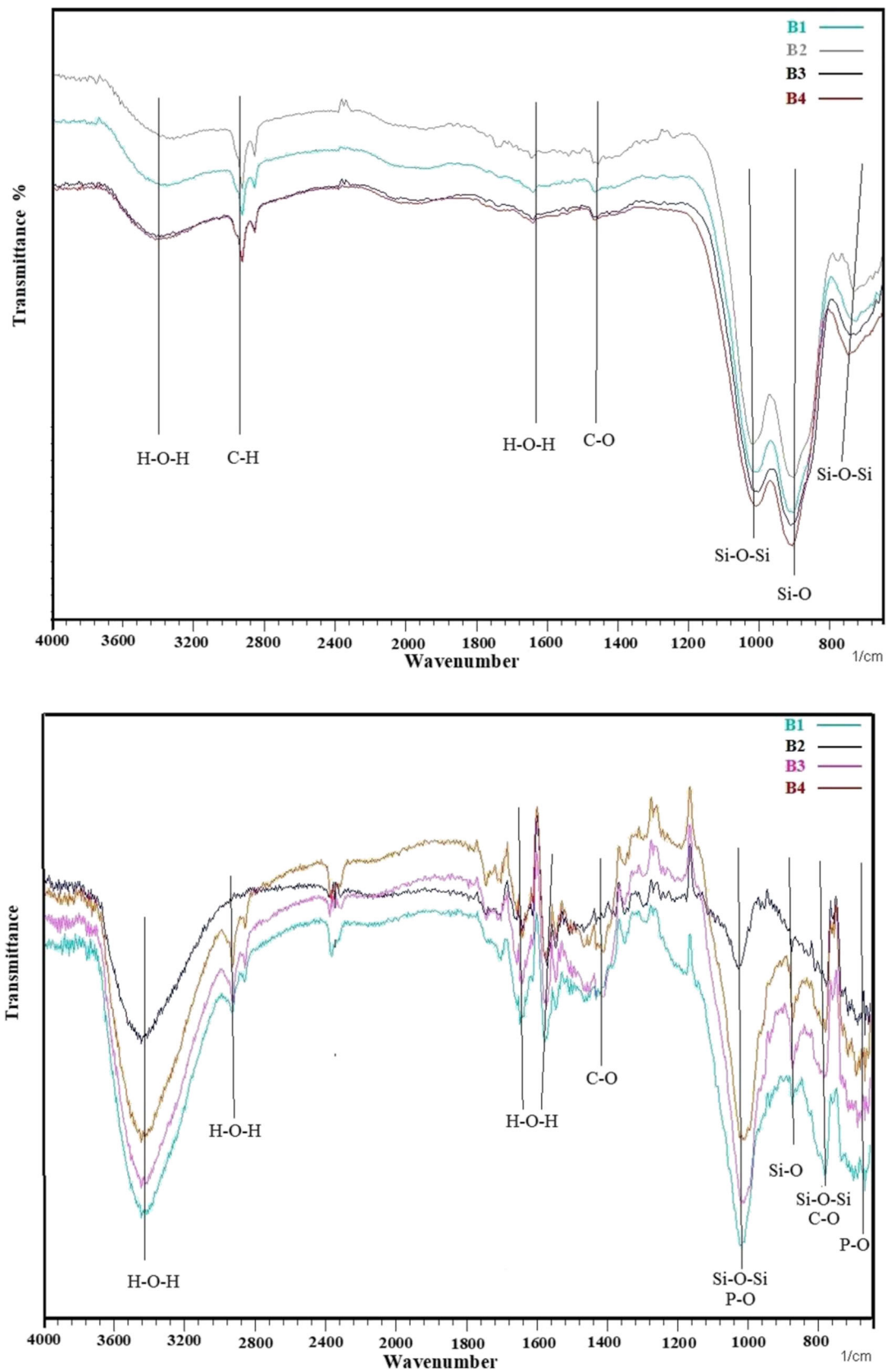


Fig. 3 FTIR spectra of samples a before SBF incubation and b after SBF incubation

Fig. 4 The weight loss (%) of the bioglasses after immersion in SBF and TRIS

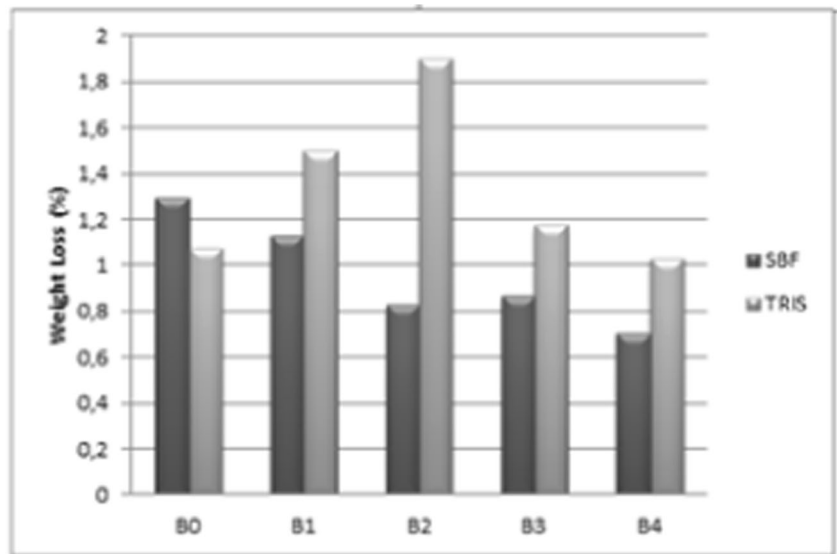


Fig. 5 The pH variation of the TRIS solution after immersion of the bioglasses within 1–7 days

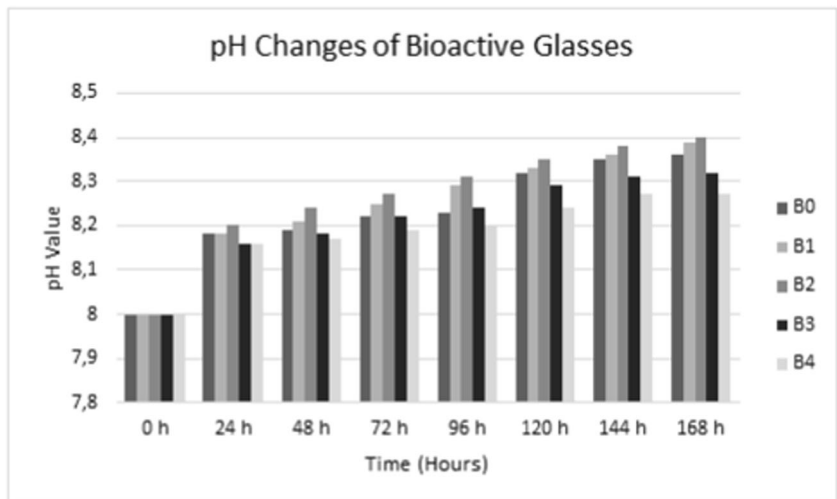


Fig. 6 The variation of microhardness values of the bioactive glass samples after immersion in SBF

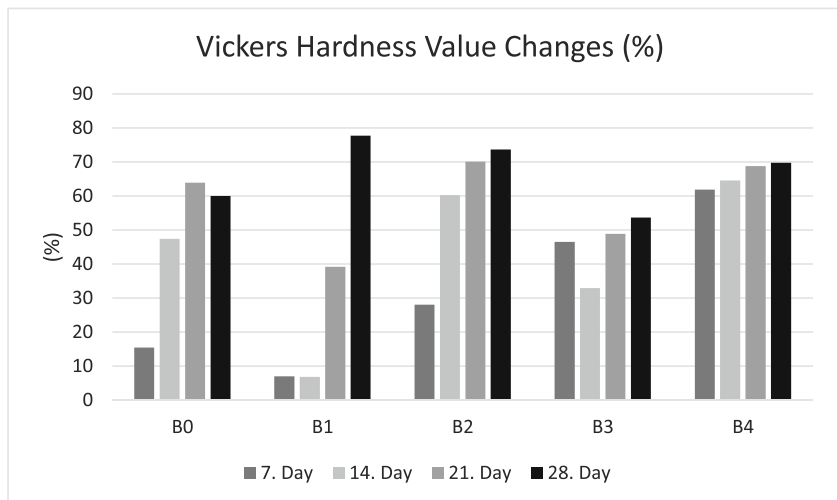


Table 2 Data of the Vickers hardness (HV) for bioactive glass samples before and after immersion in SBF

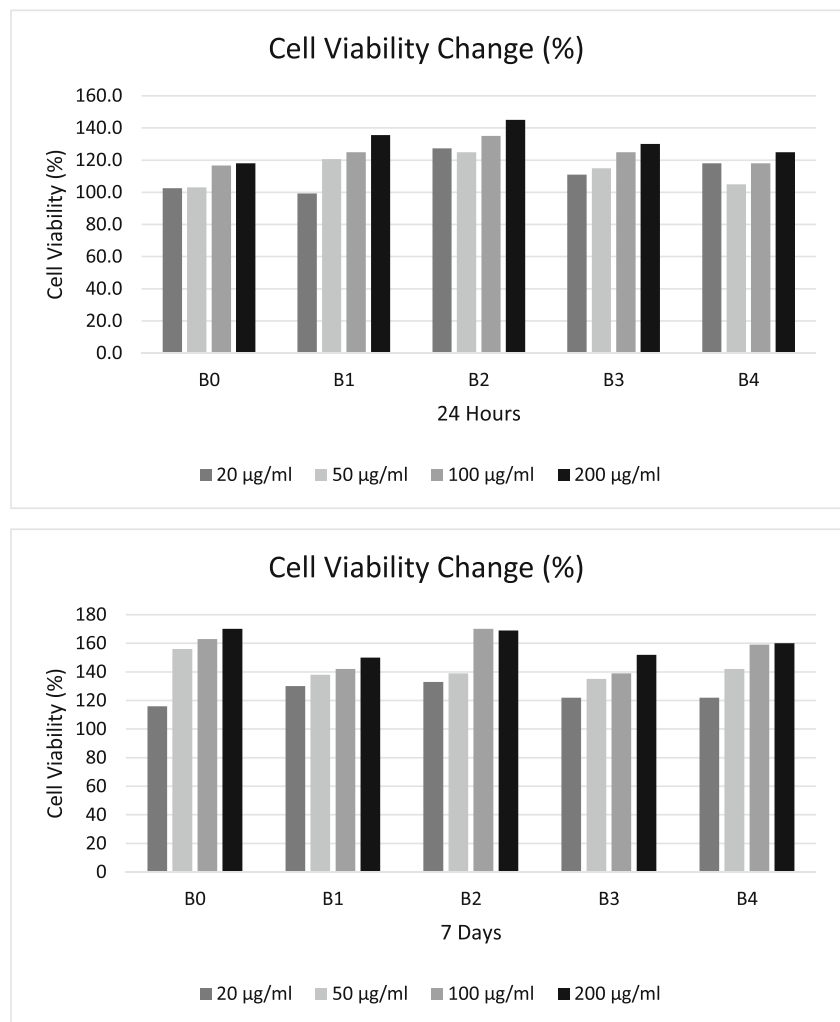
Sample	HV (kg/mm ²) before SBF	HV (kg/mm ²) after immersion in SBF			
		7 days	14 days	21 days	28 days
B0	378 (46.4)	319 (63.7)	198 (45.6)	136 (92.6)	151(75.5)
B1	504 (74.0)	401 (33.0)	386 (52.9)	268 (51.0)	132 (10.3)
B2	545 (64.0)	392 (67.8)	216 (52.7)	162 (41.1)	138 (7.4)
B3	495 (56.6)	222 (51.2)	215 (55.1)	182 (45.3)	116 (48.9)
B4	519 (57.2)	198 (12.2)	184 (36.8)	162 (46.1)	170 (21.9)

The results were given as mean ± standard deviation

release was faster at first 24–48 h and continued slowly. Similar results were found by Posti et al. [40], Siqueira et al. [41], and Essien et al. [42]. The order of the pH increase of TRIS solution from the highest to the lowest was B1 = B2, B0, B3, B4 bioactive glass sample, respectively. It is remarkable that the incorporation of 0.75 and 1.5 wt.% selenium had a positive effect on the bioactivity of bioglasses; however, the

addition of selenium more than 1.5 wt.% had not any positive effect. The pH variation results were in agreement with the weight variation results. Moreover, the final pH values (8.4) are well-nigh to the reference [41]. Siqueira et al. [41] observed that the final pH values around 8.2 after 6 days of exposure of SiO₂-CaO-Na₂O-P₂O₅ bioactive powders to SBF solution.

Fig. 7 The MTT assay results for in vitro biocompatibility of bioglass samples



Vickers hardness analysis of bioactive glass samples

The variations of hardness were measured to observe the change of the hardness of samples after immersion in SBF for different time periods. Figure 6 and Table 2 illustrate the fall in microhardness values of the samples.

It was determined that selenium incorporation increased the Vickers hardness of bioactive glasses due to the exchange of a lighter cation (Na_2O) by a denser one (SeO_2). This indicates that the bioglasses might show better long-term stability in the biological environment [29]. However, there was no correlation between

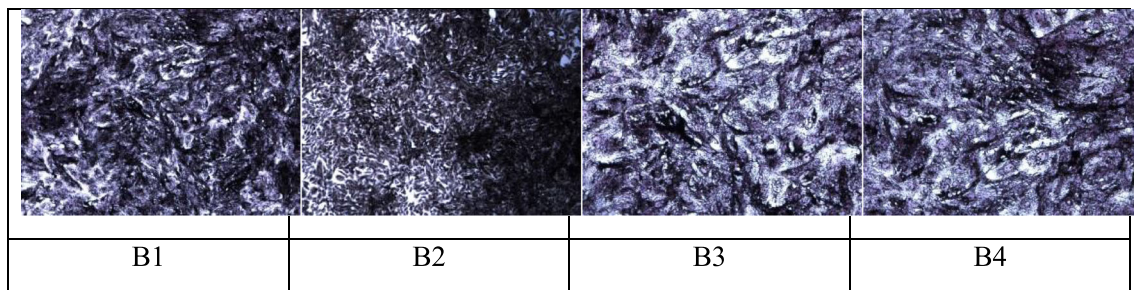
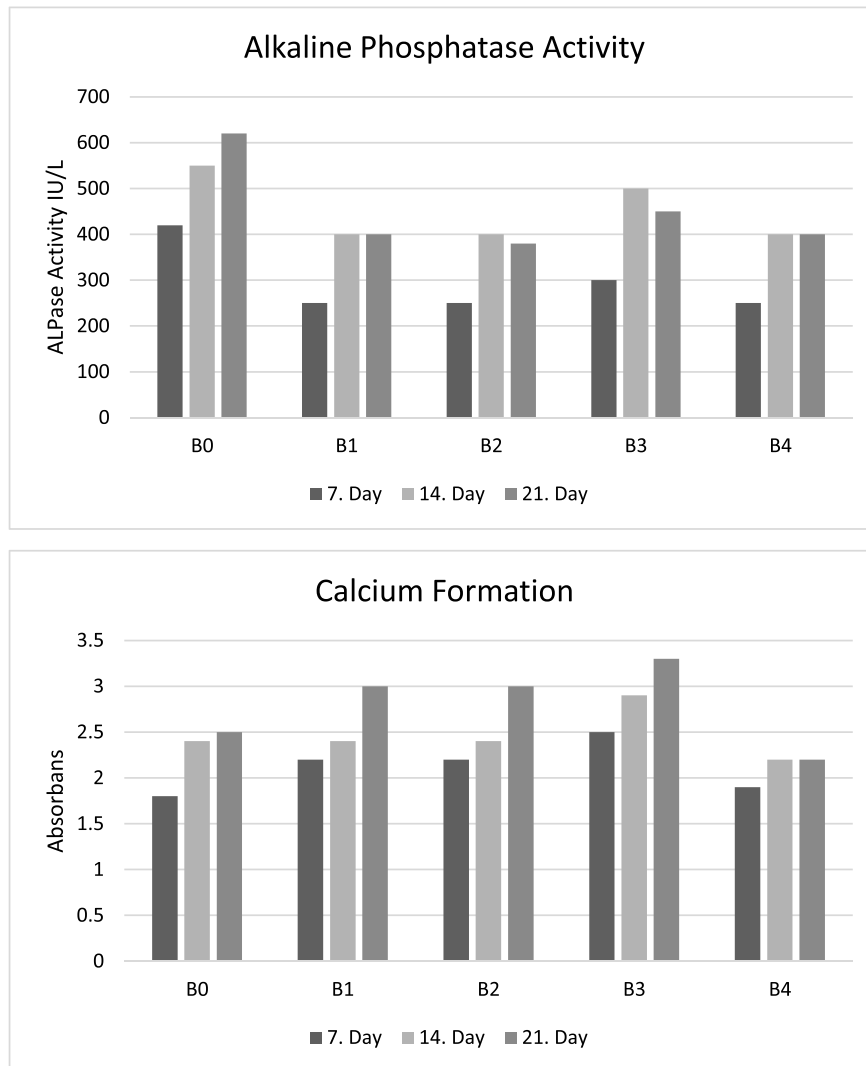


Fig. 8 Histograms of **a** alkaline phosphatase activity of SAOS-2 cells in the presence of bioglasses, **b** variation of calcium formation, and **c** microscopy results of calcium formation

the value of increase in added selenium ratio and the value of increase in Vickers hardness according to the ANOVA results. The microhardness value varies from 378 to 545 HV. The standard deviation of the measurements varies from 7.4 to 92.6. Particularly, B2 sample (1.5 wt.% SeO₂) had the best microhardness (545 (64.0) kg/mm²).

Cannillo et al. [43] reported that 45S5 (45 wt.% SiO₂, 6 wt.% P₂O₅, 24.5 wt.% Na₂O, 24.5 wt.% CaO) bioglass had a 474.1 (46.4) microhardness value. Yücel et al. [22] recorded a Vickers microhardness of 445 HV for strontium-doped 45S5 bioglass (45 wt.% SiO₂, 24.5 wt.% Na₂O, 14 wt.% CaO, 6 wt.% P₂O₅, and 10.5 wt.% SrO). The microhardness values of selenium-incorporated bioglasses obtained in this study were relatively higher than the values reported for 45S5 bioglasses.

The measurements of Vickers hardness demonstrated that the values of hardness decrease as immersion time increases. It is related with the degradation of Ca²⁺ and Na⁺ ions from bioglass that interacts with (PO₄)³⁻ ions in SBF and leads to the precipitation of HCA on the surface of the glass samples. At the same time, the value of the Vickers hardness gives information about the bioactivity of glasses. Because the HCA layer formation on the surface of glass depends on the bioactivity of glass. The Vickers hardness of samples decreases gradually due to the increase of HCA layer. The decrease of hardness was faster at the initial days due to higher dissolution rates. In the following weeks, it decelerated because of the gradual reduction in dissolution rate and the permanent precipitation.

After 28 days of immersion in SBF, B2 bioactive glass showed the highest reduction between samples. Thus, it was observed that the B2 sample showed the highest bioactivity.

Cell study results

Cell viability results

MTT assay was used to determine the cell viability percentage of the bioglass samples at different concentrations. The results are given in histogram (Fig. 7). There were significant differences in cell viability between the samples. After 24 h of incubation, an increase in cell viability was observed in the all samples. After 7 days of incubation, the B2 sample showed better biocompatibility when compared to B1, B3, and B4. In addition, the cell viability percentages of B0 and B2 sample were found to be similar at the end of 7 days.

Mineralization and alkaline phosphatase activity

It is approved that alkaline phosphatase is a biochemical marker of osteoblasts and early osteogenic

differentiation [44]. The alkaline phosphatase activity and mineralization results are demonstrated in Fig. 8. Lower alkaline phosphatase activity was observed in all samples as compared to selenium-free sample (B0). This may indicate that the bone formation was lower for selenium-incorporated samples. However, selenium incorporation enhanced the mineralization process. All selenium-incorporated bioglass samples showed better calcium formation than the pure sample.

Conclusions

Melt-derived 45S5 bioactive glasses with and without SeO₂ addition with five different compositions were prepared in order to determine the effect of selenium addition on the bioactivity, biodegradability, and biocompatibility behavior of glasses. The results of SEM study showed that, especially after 14- and 28-day immersion in SBF, the surface morphology of the glasses changed remarkably, from a plate-like structure to circular structure. Results from the ICP study suggested that carbonate-containing calcium phosphate layer would be observed on the samples. Consistent with the results of SEM micrographs, the data of FT-IR and ICP analysis, the behavior of the samples immersed in TRIS–HCl solutions represented that the SiO₂–CaO–Na₂O–P₂O₅–SeO₂ glass systems were bioactive materials. Despite the other selenium-incorporated bioglasses, partially 1.5 wt.% selenium-incorporated glass (B2) showed better bioactivity. The results showed that the selenium incorporation strengthened the bioglass structure, raised the Vickers hardness, and consequently enhanced the mechanical property. Additionally, selenium incorporation enhanced the mineralization process. Based on the outputs of this study, selenium-incorporated bioglass seems to be a promising candidate for bone tissue engineering applications. Further studies will be undertaken to evaluate selenium-incorporated 45S5 bioglass for bone cancer therapy.

Funding information The TUBITAK (The Scientific and Technological Research Council of Turkey) provided financial support through a 3001 project (Project No: 21M647).

References

- Gatti, A.M., Valdre, G., Tombesi, A.J.: Importance of microanalysis in understanding mechanism of transformation in active glassy biomaterials. *J. Biomed. Mater. Res.* **31**, 475 (1996)
- Jallot, E., Benhayoune, H., Kilian, L., Irigaray, J.L., Oudadesse, H., Balossier, G., Bonhomme, P.: STEM and EDXS characterization of

- physicochemical reactions at the interface between a bioglass coating and bone. *Surf. Interface Anal.* **29**, 314–320 (2000)
3. Qiu, Q.Q., Ducheyne, P., Ayyaswamy, P.S.: New bioactive, degradable composite microspheres as tissue engineering substrates. *J. Biomed. Mater. Res.* **52**, 66–76 (2000)
 4. Hench, L.L., Splinter, R.J., Greenlee, T.K., et al.: Bonding mechanisms at the interface of ceramic prosthetic materials. *J. Biomed. Mater. Res.* **5**, 117–141 (1971)
 5. Kitsugi, T., Nakamura, T., Oka, M., Senaha, Y., Goto, T., Shibuya, T.: Bone-bonding behavior of plasma-sprayed coatings of bioglass, AW-glass ceramic, and tricalcium phosphate on titanium alloy. *J. Biomed. Mater. Res.* **30**, 261–269 (1996)
 6. Hench, L.L., Thompson, I.: Twenty-first century challenges for biomaterials. *J. R. Soc. Interface.* **7**, 379–391 (2010)
 7. Hench, L.L., West, J.K.: Biological applications of bioactive glasses. *Life Chem. Rep.* **13**, 187–241 (1996)
 8. Melchers, S., Uesbeck, P., Winter, O., Eckert, H., Eder, D.: Effect of aluminum ion incorporation on the bioactivity and structure in mesoporous bioactive glasses. *Chem. Mater.* **28**, 3254–3264 (2016)
 9. Yang, X., Zhang, L., Chen, X., Sun, X., Yang, G., Guo, X.H., Yang, H., Gao, C., Gou, Z.: Incorporation of B₂O₃ in CaO-SiO₂-P₂O₅ bioactive glass system for improving strength of low-temperature co-fired porous glass ceramics. *J. Non-Cryst. Solids.* **358**, 1171–1179 (2012)
 10. Wu, C.T., Zhou, Y.H., Xu, M.C., Han, P., Chen, L., Chang, J., Xiao, Y.: Copper-containing mesoporous bioactive glass scaffolds with multifunctional properties of angiogenesis capacity, osteostimulation and antibacterial activity. *Biomater.* **34**, 422–433 (2013)
 11. Goel, A., Rajagopal, R.R., Ferreira, J.M.F.: Influence of strontium on structure, sintering and biodegradation behavior of CaO-MgO-SrO-SiO₂-P₂O₅-CaF₂ glasses. *Acta Biomater.* **7**, 4071–4080 (2011)
 12. Lao, J., Jallot, E., Nedelec, J.M.: Strontium-delivering glasses with enhanced bioactivity: a new biomaterial for Antiosteoporotic applications? *Chem. Mater.* **20**, 4969–4973 (2008)
 13. Wang, X., Zhang, Y., Ma, Y., Chen, D., Yang, H., Li, M.: Selenium-containing mesoporous bioactive glass particles: physicochemical and drug delivery properties. *Ceram. Int.* **42**, 3609–3617 (2016)
 14. Rodríguez-Valencia, C., López-Álvarez, M., Cochón-Cores, B., Pereiro, I., Serra, J., González, P.: Novel selenium-doped hydroxyapatite coatings for biomedical applications. *J. Biomed. Mater. Res. A.* **101A**, 853–861 (2013)
 15. Li, Y.H., Li, X.L., Wong, Y.S., Chen, T., Zhang, H., Liu, C., Zheng, W.: The reversal of cisplatin-induced nephrotoxicity by selenium nanoparticles functionalized with 11-mercapto-1-undecanol by inhibition of ROS-mediated apoptosis. *Biomater.* **32**, 9068–9076 (2011)
 16. Tran, P.A., Sarin, L., Hurt, R.H., Webster, T.J.: Titanium surfaces with adherent selenium nanoclusters as a novel anticancer orthopedic material. *J. Biomed. Mater. Res. A.* **93**(4), 1417–1428 (2010). <https://doi.org/10.1002/jbm.a.32631>.
 17. Torres, S.K., Campos, V.L., León, C.G., Rodríguez-Llamazares, S.M., Rojas, S.M., González, M., Smith, C., Mondaca, M.A.: Biosynthesis of selenium nanoparticles by *Pantoea* agglomerans and their antioxidant activity. *J. Nanopart. Res.* **14**, 1–9 (2012)
 18. Ma, J., Wang, Y.H., Zhou, L., Zhang, S.: Preparation and characterization of selenite substituted hydroxyapatite. *Mater. Sci. Eng. C.* **33**, 440–445 (2013)
 19. Tran, P., Webster, T.J.: Enhanced osteoblast adhesion on nanostructured selenium compacts for anti-cancer orthopedic applications. *Int. J. Nanomedicine.* **3**, 391–396 (2008)
 20. Kokubo, T.: Advanced series in ceramics. In: Hench, L.L., Wilson, J. (eds.) *An Introduction to Bioceramics*, vol. 1, pp. 75–88. World Sci, Singapore (1993)
 21. Taş, A.C.: Synthesis of biomimetic Ca-hydroxyapatite powders at 37°C in synthetic body fluids. *Biomater.* **211**, 429–438 (2000)
 22. Yücel, S., Terzioğlu, P., Aydın-Sinirlioğlu, Z., Tekerek, B.S., Basaran-Elalmis, Y.: Synthesis, characterization, in vitro degradability and bioactivity of strontium substituted Rice Hull ash silica based melt derived 45S5 bioactive glass. *Sigma J Eng. Natur. Sci.* **33**, 23–32 (2015)
 23. Kokubo, T., Takadama, H.: How useful is SBF in predicting in vivo bone bioactivity? *Biomaterials.* **27**, 2907–2915 (2006)
 24. Guerrero-Lecuona, M.C., Canillas, M., Pena, P., Rodríguez, M.A., De Aza, D.H.: Different in vitro behavior of two Ca₃(PO₄)₂ based biomaterials, a glass-ceramic and a ceramic, having the same chemical composition. *Bol. Soc. Esp. Ceram. V.* **54**, 181–188 (2015)
 25. Arepalli, S.K., Tripathi, H., Hira, S.K., Manna, P.P., Pyare, R., Singh, S.P.: Enhanced bioactivity, biocompatibility and mechanical behavior of strontium substituted bioactive glasses. *Mater. Sci. Eng. C.* **69**, 108–116 (2016)
 26. Özarslan, A.C., Yücel, S.: Fabrication and characterization of strontium incorporated 3-D bioactive glass scaffolds for bone tissue from biosilica. *Mater. Sci. Eng. C.* **68**, 350–357 (2016)
 27. Yucel, S., Özçimen, D., Terzioğlu, P., Acar, S., Yaman, C.: Preparation of melt derived 45S5 bioactive Glass from Rice Hull ash and its characterization. *Adv. Sci. Lett.* **19**, 3477–3481 (2013)
 28. Souza, M.T., Crovace, M.C., Schröder, C., Eckert, H., Peitl, O., Zanotto, E.D.: Effect of magnesium ion incorporation on the thermal stability, dissolution behavior and bioactivity in bioglass-derived glasses. *J. Non-Cryst. Solids.* **382**, 57–65 (2013)
 29. Gu, Y.W., Khor, K.A., Cheang, P.: In vitro studies of plasma-sprayed hydroxyapatite/Ti-6Al-4V composite coatings in simulated body fluid (SBF). *Biomater.* **24**, 1603–1611 (2003)
 30. Kokubo, T., Ito, S., Shigematsu, M., Sanka, S., Yamamuro, T.: Fatigue and life-time of bioactive glass-ceramic A-W containing apatite and wollastonite. *J. Mater. Sci.* **22**, 4067–4070 (1987)
 31. Bohner, M., Lemaître, J.: Can bioactivity be tested in vitro with SBF solution? *Biomater.* **30**, 2175–2179 (2009)
 32. Yan, H., Zhang, K., Blanford, C.F., Francis, L.F., Stein, A.: In vitro Hydroxycarbonate apatite mineralization of CaO-SiO₂ sol-gel glasses with a three-dimensionally ordered macroporous structure. *Chem. Mater.* **13**, 1374–1382 (2001)
 33. Mansur, H.S., Costa, H.S.: Nanostructured poly(vinyl alcohol)/ bioactive glass and poly(vinyl alcohol)/chitosan/ bioactive glass hybrid scaffolds for biomedical applications. *Chem. Eng. J.* **137**, 72–83 (2008)
 34. Hesaraki, S., Alizadeh, M., Nazarian, H., Sharifi, D.: Physicochemical and in vitro biological evaluation of strontium/calcium Silicophosphate glass. *J. Mater. Sci. Mater. Med.* **21**, 695–705 (2010)
 35. Rezaei, Y., Moztaezadeh, F., Shahabi, S., Tahriri, M.: Synthesis, characterization, and in vitro bioactivity of sol-gel-derived SiO₂-CaO-P₂O₅-MgO-SrO bioactive glass. *Synth. React. Inorg., Met.-Org., Nano-Met. Chem.* **44**, 692–701 (2014)
 36. Varila, L., Fagerlund, S., Lehtonen, T., Tuominen, J., Hupa, L.: Surface reactions of bioactive glasses in buffered solutions. *J. Eur. Ceram. Soc.* **32**, 2757–2763 (2012)
 37. Cerrutia, M.G., Greenspan, D., Powers, K.: An analytical model for the dissolution of different particle size samples of bioglass in TRIS-buffered solution. *Biomater.* **26**, 4903–4911 (2005)
 38. Saboori, A., Rabiee, M., Moztaezadeh, F., Sheikhi, M., Tahriri, M., Karimi, M.: Synthesis, characterization and in vitro bioactivity of sol-gel-derived SiO₂-CaO-P₂O₅-MgO bioglass. *Mater. Sci. Eng. C.* **29**, 335–340 (2009)
 39. Nayak, J.P., Kumar, S., Bera, J.: Sol-gel synthesis of bioglass-ceramics using rice husk ash as a source for silica and its characterization. *J. Non-Cryst. Solids.* **356**, 1447–1451 (2010)
 40. Posti, J.P., Piitulainen, J.M., Hupa, L., Fagerlund, S., Frantzen, J., Aitasalo, K.M.J., Vuorinen, V., Serlo, W., Syrjänen, S., Vallittu,

- P.K.: A glass fiber-reinforced composite- bioactive glass cranioplasty implant: a case study of an early development stage implant removed due to a late infection. *J. Mech. Behav. Biomed. Mater.* **55**, 191–200 (2015)
41. Siqueira, R.L., Peitl, O., Zanutto, E.: Gel-derived $\text{SiO}_2\text{-CaO-Na}_2\text{O-P}_2\text{O}_5$ bioactive powders: synthesis and in vitro bioactivity. *Mater. Sci. Eng.* **31**, 983–991 (2011)
42. Essien, E.R., Adams, L.A., Shaibu, R.O., Olasupo, I.A., Oki, A.: Economic route to sodium-containing silicate bioactive glass scaffold. *Open J Regen. Med.* **1**, 33–40 (2012)
43. Cannillo, V., Chiellini, F., Fabbri, P., Sola, A.: Production of bioglass® 45S5 Polycaprolactone composite scaffolds via salt-leaching. *Compos. Struct.* **92**, 1823–1832 (2010)
44. Wan, Y., Cui, T., Li, W., Li, C., Xiao, J., Zhu, Y., Ji, D., Xiong, G., Luo, H.: Mechanical and biological properties of bioglass/magnesium composites prepared via microwave sintering route. *Mater. Des.* **99**, 521–527 (2016)

Publisher's note Springer Nature remains neutral with regard to jurisdictional claims in published maps and institutional affiliations.